

# DRUG AND METABOLITES STUDY IN WHOLE BODY ANIMAL BY HIGH DEFINITION MALDI IMAGING

*Paul Murray<sup>1</sup>, Emmanuelle Claude<sup>1</sup>, Mark Towers<sup>1</sup>, Ian Edwards<sup>1</sup>, Lars Bendahl<sup>2</sup>, Joahnnes P.C. Vissers<sup>1</sup>*  
<sup>1</sup> Waters Corporation, Manchester, UK, <sup>2</sup> H. Lundbeck A/S Denmark

## INTRODUCTION

**Mass spectrometry Imaging (MSI) is increasingly used in pharmacokinetics. It has been recognized as complementary to Whole-Body Autoradiography, which is traditionally used for approval of a drug by the Food and Drug Administration Agency.**

**There are three main advantages of MSI: Cost savings compared to the expensive requirement to radio-label the drug to be visualized in WBA; absolute confirmation that the drug is indeed visualized as the molecular ion is followed and not the labelled itself that could be attached to a metabolite; and the possibility to visualize the metabolites within the same tissue section.**

**In this study Olanzapine (OLZ) was studied. The pharmacokinetics of this drug have been intensively studied in different animals<sup>1</sup>. However, spatial distribution analysis solely by MSI lacks specific information. Typically, drug distribution analysis by MSI is conducted by using a targeted MS/MS analysis method for the drug of interest, aiming to achieve better sensitivity and specificity.**

**In this study, a multiplex targeted approach was evaluated and untargeted MSI analysis experiment explored, where OLZ and its metabolites, along with endogenous molecules, are being imaged within a single whole body section.**

## METHODS

### Sample preparation

Olanzapine (OLZ) was administrated by oral gavage to male Lister-Hooded rats at 8 mg/kg. Animals were euthanized at 2 or 6 hours post-dose. 30-µm-thick whole-body sagittal tissue sections were mounted on invisible mending tape. A single section of a whole rat spanned three MALDI plates. A solution of α-cyano-4-hydroxycinnamic acid matrix at 5 mg/mL was applied evenly to the sample in several coats using a SunCollect nebulising spray device.

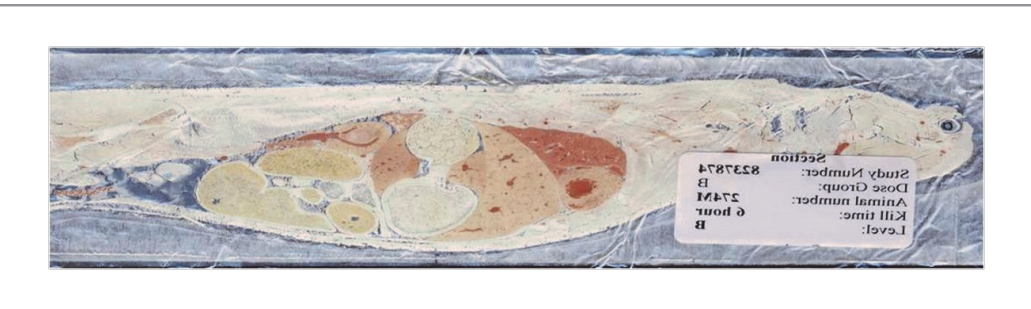


Figure 1. Rat whole-body sagittal tissue section photographic image.

TO DOWNLOAD A COPY OF THIS POSTER, VISIT [WWW.WATERS.COM/POSTERS](http://WWW.WATERS.COM/POSTERS)

### Mass Spectrometry

Data were acquired using a MALDI SYNAPT G2 mass spectrometer in MS and MS/MS mode with tri-wave ion guide optics to separate ions according to their ionic mobility in the gas phase.

### MALDI-MS

Laser: solid state Nd:YAG laser (λ = 355nm)  
Pulse rate: 1000 Hz  
Spatial resolution: 400 µm (lateral)  
IMS pressure: 3.3 mBar  
Wave height: 40 V  
Wave velocity: 750 to 250 m/s

MS conditions: Mass Range: 50-600 Da  
MS/MS conditions: High duty cycle on for sensitivity improvement  
Collision energy 35 eV

The obtained data sets were subsequently processed using High Definition Imaging (HDI) MALDI software for detailed image analysis.

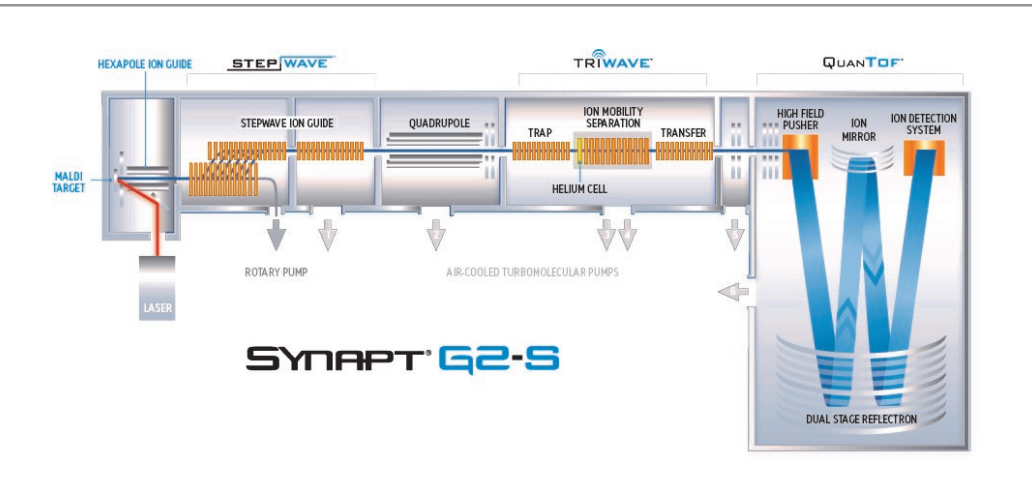


Figure 2. Schematic of the MALDI SYNAPT G2.

## RESULTS

### Targeted Multiplex MS/MS MALDI imaging experiment

A first experiment was carried out on the 2 h post-dose tissue section in a multiplex targeted MS/MS approach where the drug and the two known metabolites were MALDI imaged from a single tissue section. (Figure 3). The acquisition was carried out in High Duty Cycle mode on to improve the sensitivity of the detection of the three compounds fragments.

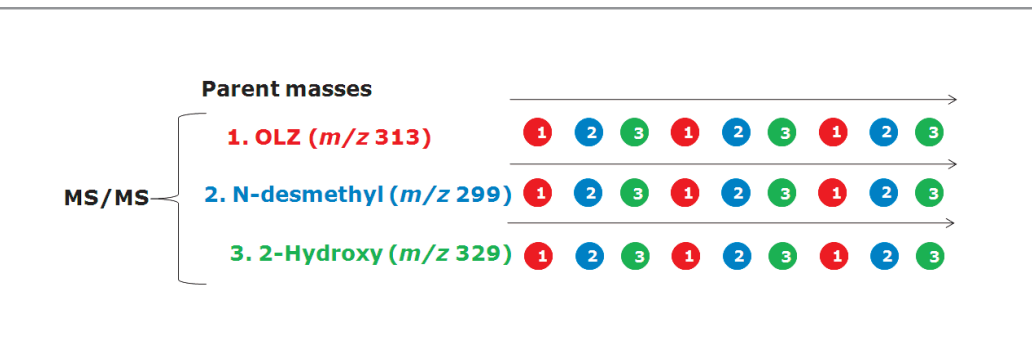


Figure 3. Schematic of the multiplexed MS/MS MALDI imaging experiment.

Figure 4 displays the fragment specific ion images obtained from the multiplexed MS/MS experiment, illustrating distinct different distribution of the three compounds of interest.

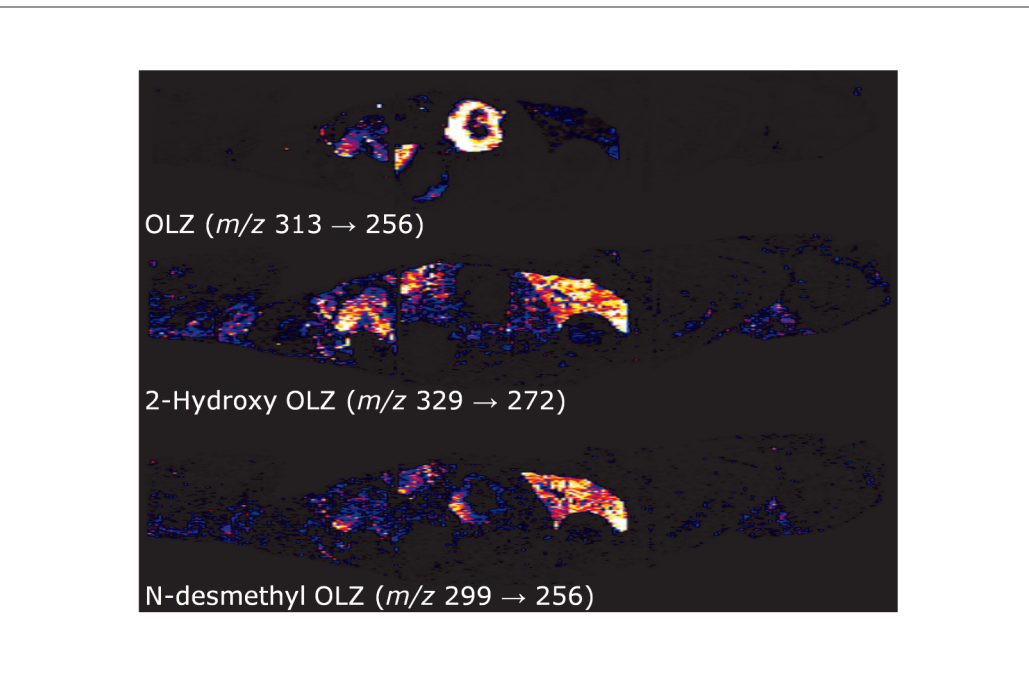


Figure 4. Fragment specific ion images for the multiplexed MS/MS experiment .

### Untargeted IMS-MS MALDI imaging experiment

#### OLZ plus two metabolites distributions

A second experiment was performed on the 6 h post-dose tissue section in untargeted MS mode. In this instance, ion mobility separation was used to add specificity to the experiment. The drug and the two main metabolites were imaged (Figure 5). From the HDI software, the raw data were processed and peak detected using Apex3D. Each detected peak is reported with an intensity, a *m/z* and a specific drift time and displayed either in a spectrum view (intensity and *m/z*) and 2D-plot (*m/z* vs. drift time).

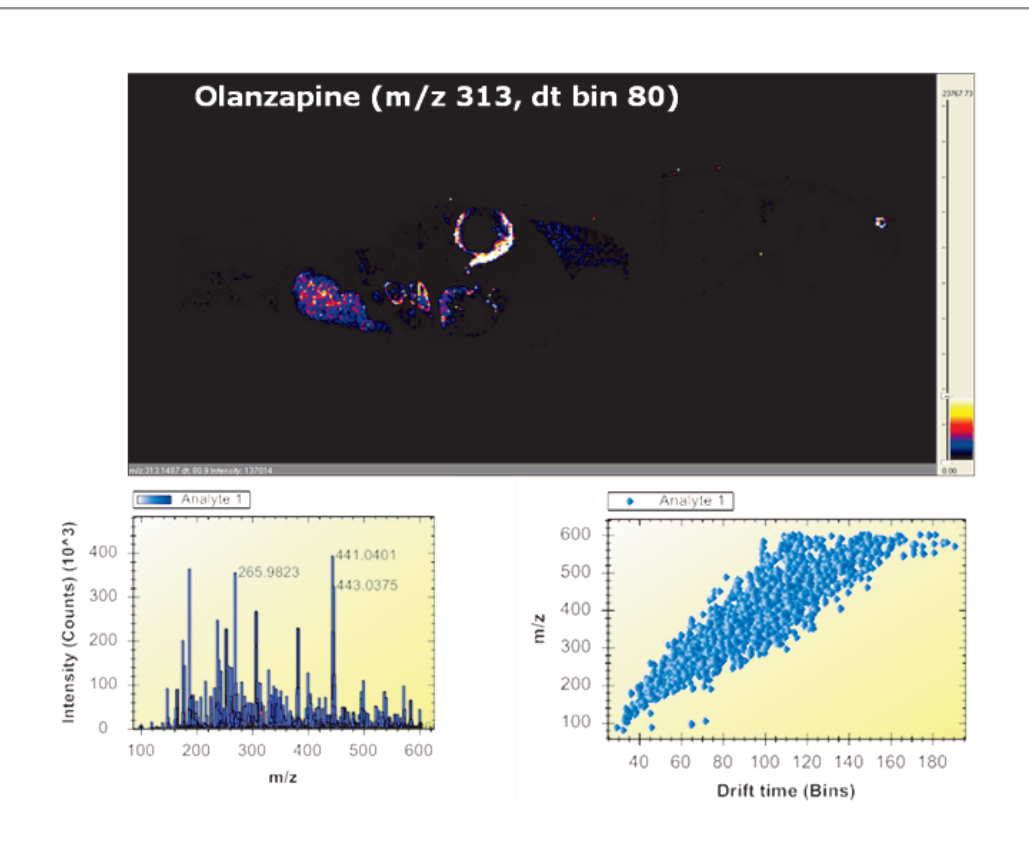


Figure 5. OLZ ion image display through High Definition Imaging (HDI) software.

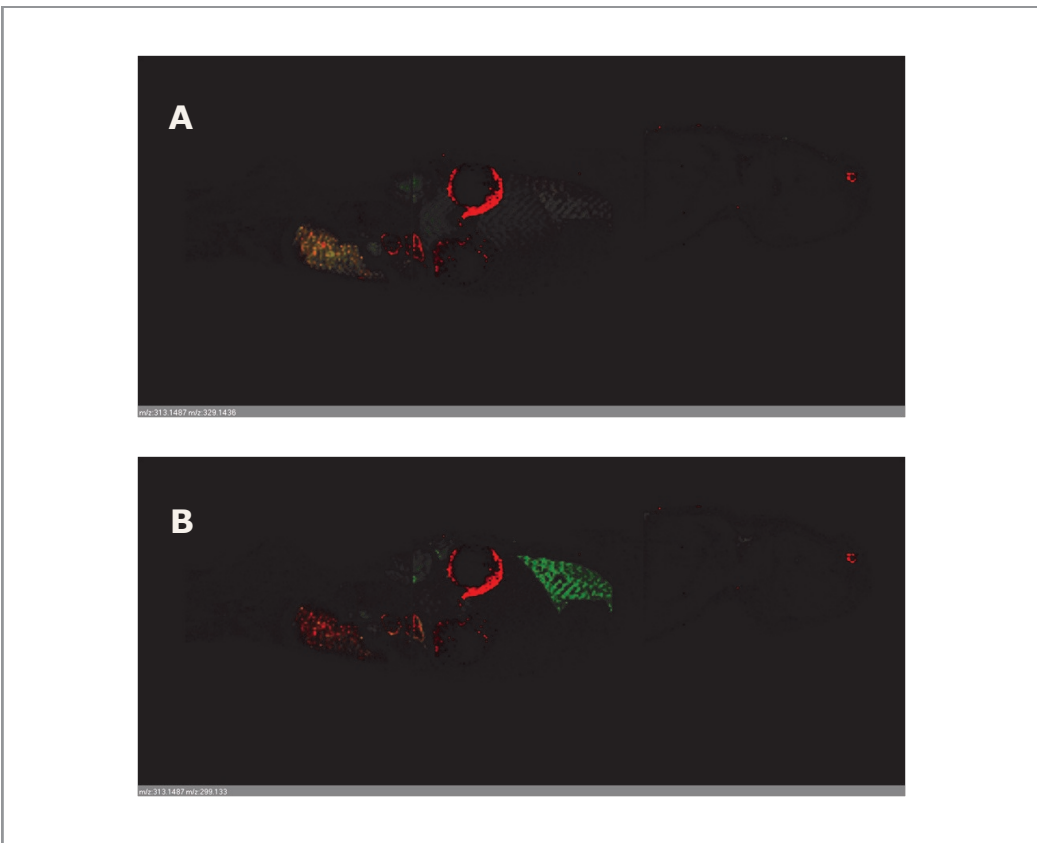


Figure 6. A: Overlay of the OLZ (*m/z* 313, red ion image) distribution with the 2-hydroxy OLZ metabolite (*m/z* 329, green ion image), B: Overlay of the OLZ (*m/z* 313, red ion image) distribution with the N-desmethyl OLZ metabolite (*m/z* 299, green ion image).

#### Isobaric endogenous species distribution

A vast amount of information is generated by the ionisation of endogenous species. Out of 3,000 peaks processed by the HDI software, 506 pairs had a difference in mass of 10 mDa, but their drift mobility was significantly different. The resolving power between two species in the mass range of 200 to 600 Da typically varied from 20,000 to 60,000. 212 pairs were reported with mass difference of 1 mDa or lower. In this case, the resolving power needed to differentiate species without IMS would be 200,000 to 600,000 in the same mass range. As an example, within a 1 Da window around 546.5, seven species were peak detected using the Apex3D algorithm in the HDI software. The three most abundant ones are *m/z* 546.14 and two at 546.36 In Figure 7, two isobaric ion images at *m/z* 546.36 are shown.

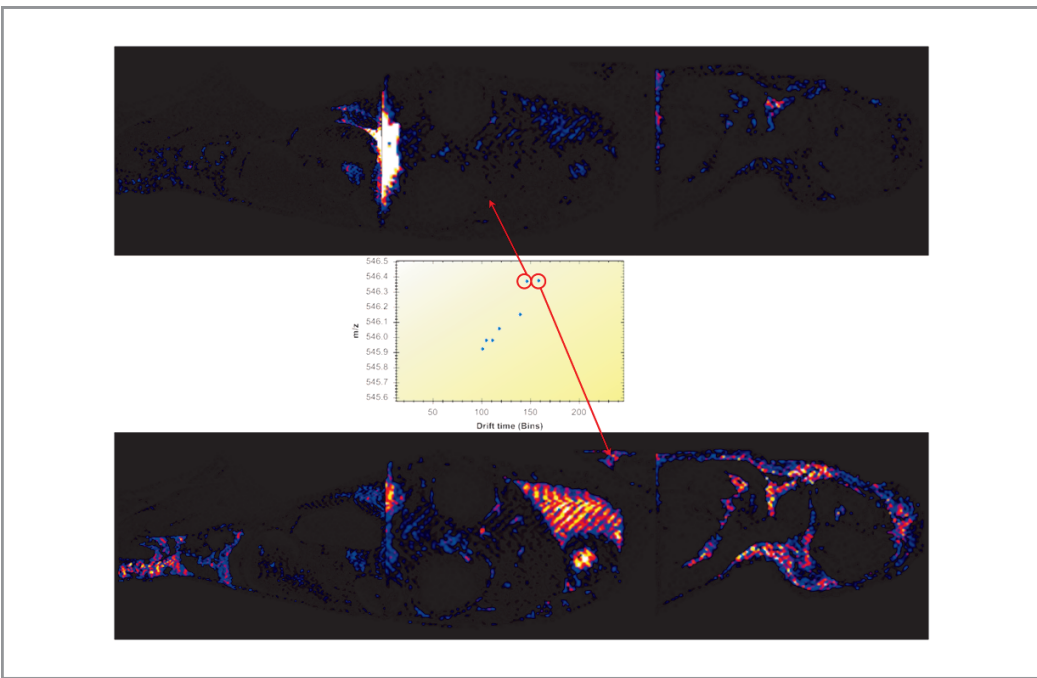


Figure 7. 2D-plot *m/z* vs. *d*, at 546.5 Da. Ion images of two isobaric species are displayed for *m/z* 546.36.

Identification of two isobaric species was attempted by conducting a manual MS/MS experiment directly from tissue where quadrupole selection window was optimised down to 1 Da (Figure 8 A)). Isobaric species were separated by ion mobility and fragmented in the Transfer T-Wave collision cell. Fragments and its respective precursor ion share the same mobility drift time. In Figure 8C, the three bands represent the selection carried out from DriftScope software to extract specific MS/MS spectra for the three species that was selected by the quadrupole.

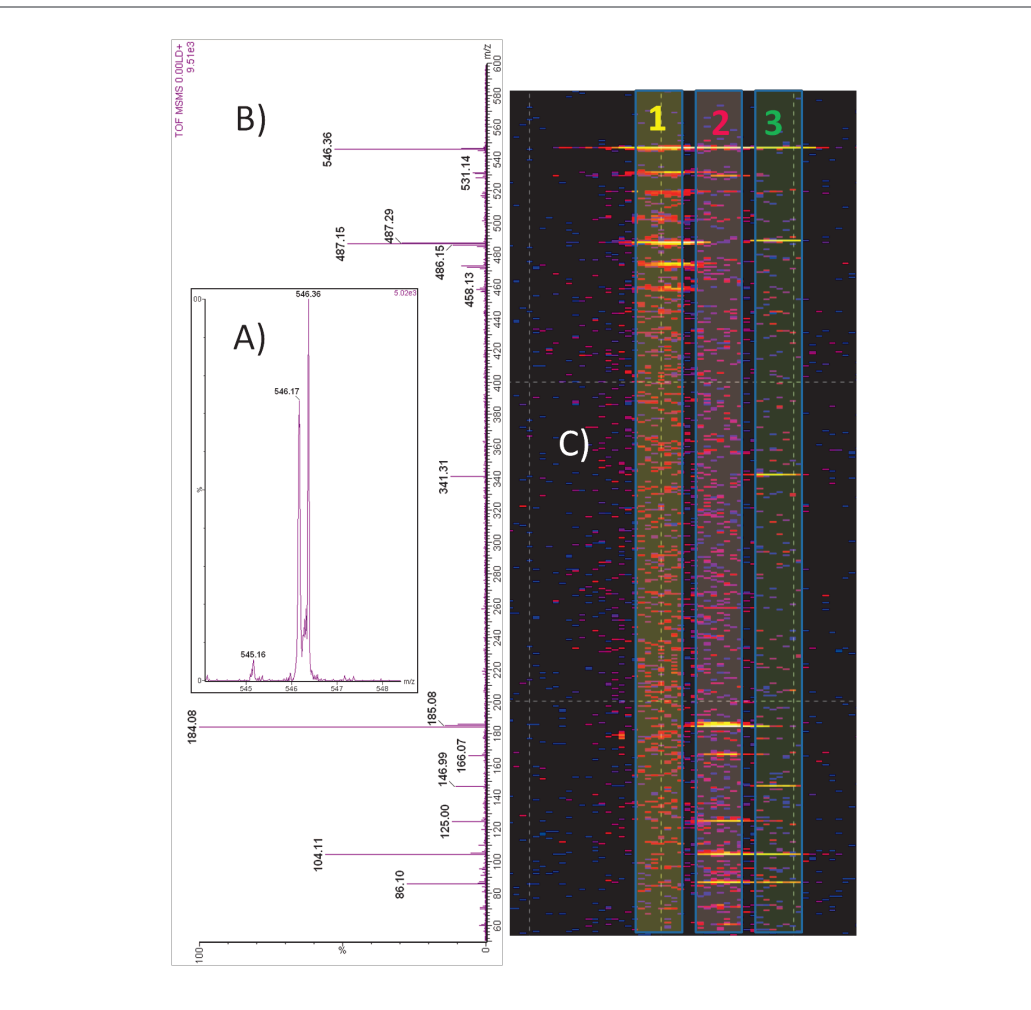


Figure 8. A) Insert showing a Q1 mass selection window of 1 Da, B) Overall MS/MS spectrum without IMS, combining the three isobaric species, C) DriftScope 2D-plot showing the transfer fragmentation vertical bands specific to each isobaric precursor.

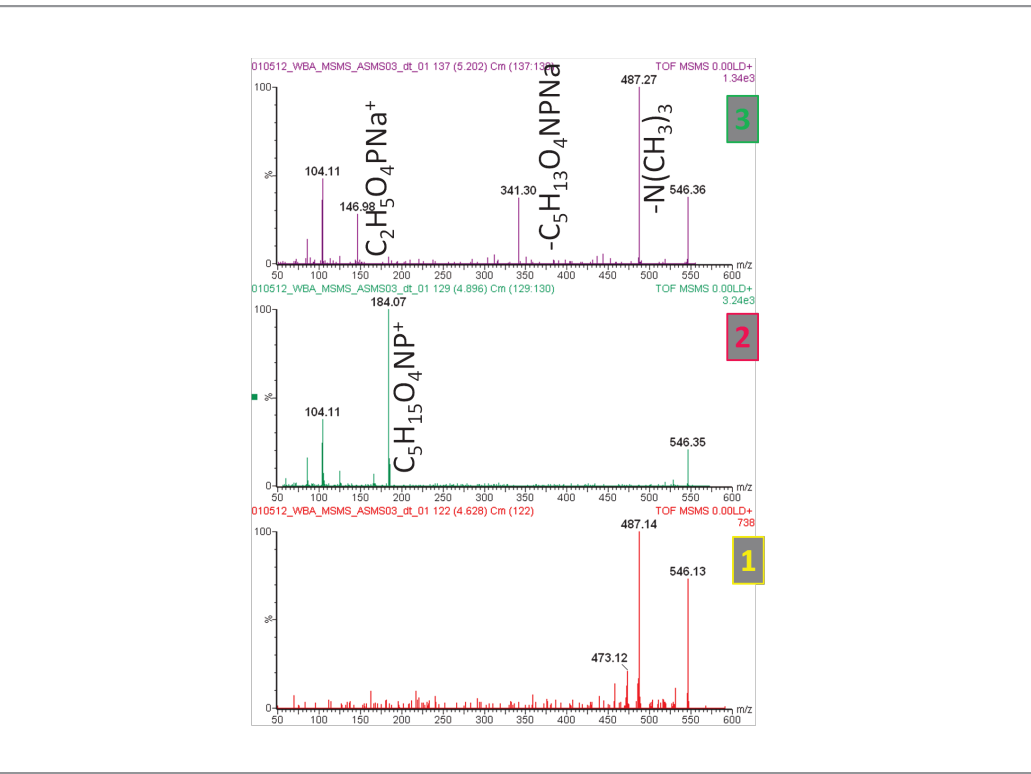


Figure 9. Drift time specific three MS/MS spectra extracted from DriftScope.

Figure 9 shows IMS specific individual MS/MS spectra. The band 1 MS/MS spectrum represents precursor ion *m/z* 546.1 and couldn't be identified. The band 2 MS/MS spectrum represents precursor ion *m/z* 546.36. A possible identification using a Lipidmaps database ([www.lipidmaps.org](http://www.lipidmaps.org)) is PC (20:3/0:0)H<sup>+</sup>. The band 3 MS/MS spectrum also represents precursor ion *m/z* 546.36. A possible identification was also made using the same database and this lipid could be PC (18:0/0:0)Na<sup>+</sup>.

Figure 10 displays four examples where pairs of isobaric species ion images were overlaid. The resolving power is calculated by dividing the *m/z* value by the *m/z* difference of the isobaric peak detected Apex3D species, illustrating the minimum resolving power needed if species could not have been separated by IMS.

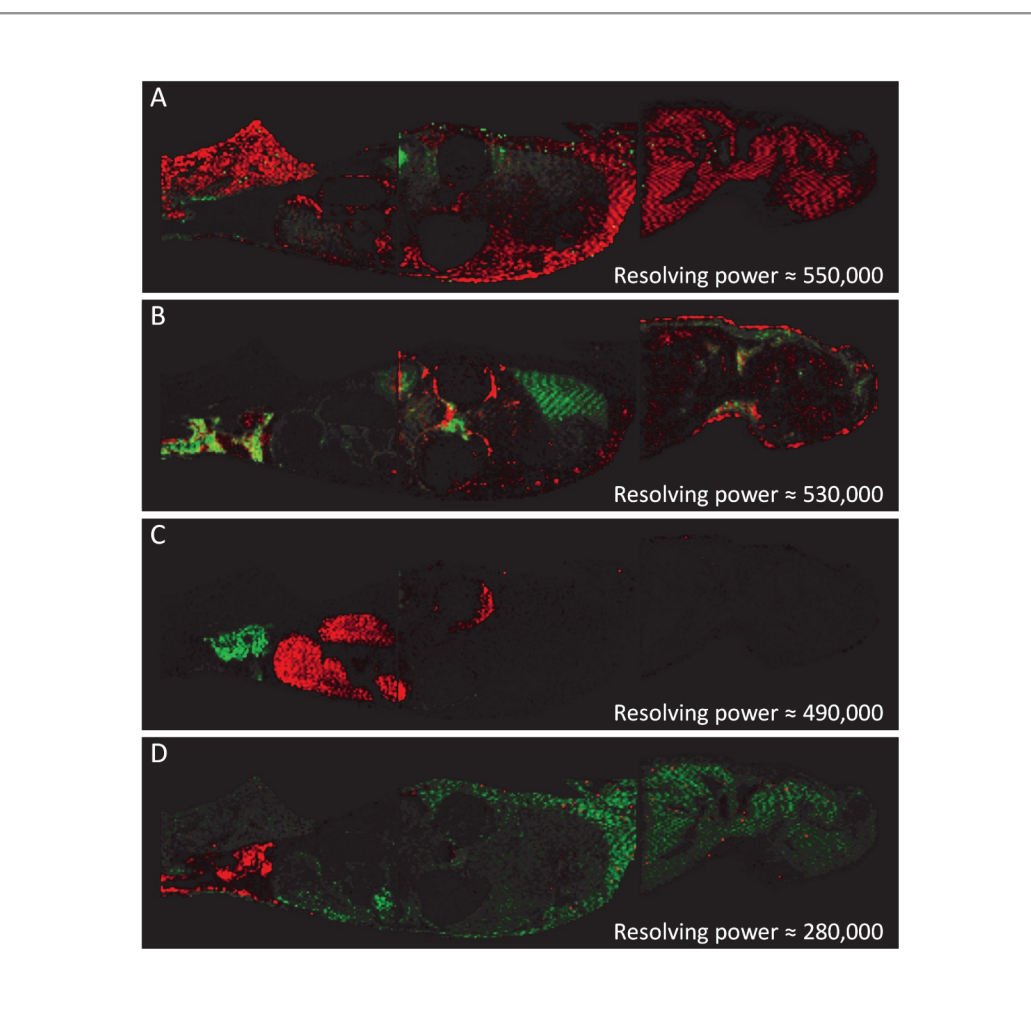


Figure 10. Overlaid ion images of isobaric species. A) Red = 331.1382, Green = 331.1388, B) Red = 370.0500, Green = 370.0507, C) Red = 296.1670, Green = 296.1676, D) Red = 303.1870, Green = 303.1098.

## CONCLUSION

- OLZ and its two main metabolites were imaged by a multiplexed MS/MS and an IMS-MS experiment
- In the IMS-MS experiment, a vast number of isobaric species were differentiated and imaged utilizing the additional specificity afforded by ion mobility
- Potential identifications of isobaric endogenous lipids were conducted directly from tissue.

### REFERENCES

1. Kelem Kassahun et al., Drug Metabolism and Disposition, 1977, Vol. 25, No. 5, pp573-583